Journal of Mines, Metals and Fuels, *70(11) : 584-589; 2022. DOI: 10.18311/jmmf/2022/32400*

Print ISSN : 0022-2755

Journal of Mines, Metals and Fuels

Contents available at: *www.informaticsjournals.com/index.php/jmmf*

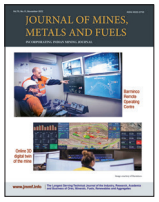

Investigation into the Blast-Induced Damage in Cut and Fill Stoping Operation

A. G. Sangode[1,2*], A. K. Raina[1], M. N. Bagde[1] and K. Ram Chandar[2]

[1]CSIR-Central Institute of Mining and Fuel Research, Nagpur Research Centre, 440001, India; agsangode@cimfr.nic.in

[2]National Institute of Technology Karnataka, Surathkal, Mangalore – 575 025, India

Abstract

The paper presents the results of a comprehensive monitoring carried out to study the extent of blast-induced damage experienced by rockmasses extracted by cut and fill stoping in a manganese mine. Damage is related to strain generated by the blasting and it is found to correlate well with the particle velocity. The particle velocities were measured in the studied mine with seismographs. The attenuation equation for extrapolation of vibration to the near field was derived from the data thus acquired. The site-specific damage model for designing the safe blast parameters was thus devised to minimize the extent of the blast-induced damage to protect the hanging wall, footwall and friable orebody and thus overall improving the stoping environment. The presented work aims at improving the understanding of the influence of blasting on the backfilled area and hard rock in the stoping environment. The damage predicted by different methods and the final strategy for blasting for wall control and productivity are documented in the paper.

Keywords: *Blast-Induced Damage, Cut and Fill Stoping, Peak Particle Velocity*

1.0 Introduction

The rockmass damage in underground mining generally occurs due to the change of induced stresses related to the mine excavation and mainly due to the blasting. As the ore is excavated, the *in-situ* stresses get re-distributed around the boundary of the openings. Since the dynamic phenomenon of loading is involved, high stresses are experienced on the back and corners of the excavations, while low stresses are generally experienced by some of the exposed stope walls. The de-stressing of the walls due to the repetitive loading, opens-up existing cracks due to the movement of the rockmass into the excavation[1,2].

During the excavation stages, it is well understood that the blast-induced damage weakens a rockmass potentially, leading to stability problems[3]. Empirical evidence from the underground stoping suggests that the near field peak particle velocity from blasting could be linked to rockmass pre-conditioning and damage[4,5]. The relationship developed between the critical peak vibration velocity and rockmass damage in the near field of the explosive-loaded blast holes was determined by correlating the measured vibrations and the damage[1]. The magnitude of the vibrations has been found to depend upon the nature of the rockmass, the explosive properties, the hole diameter used, the drilling pattern (burden, spacing, hole angle and distance of the holes to the exposed walls) and the hole deviation among others. Accordingly, vibration levels have been used to assess the damage to the rockmass due to the blasting. The study

**Author for correspondence*

presented herewith is related to the blast-induced damage and its possible effects in cut and fill stoping environment.

2.0 Experimental Set Up

This study was conducted in a manganese mine located in the northern part of the Nagpur district of Maharashtra state in India and is situated at a distance of 43.5 km from the district place Nagpur.

2.1 Description of Deposit

The S-shaped orebody in this mine is divided into 3 sections: the North limb, the South limb and the South limb extension with extremity (Figure 1). The area of the study in this paper covers the south limb extremity in-between cross-cut 8 to 11 and generally the 70-90 m wide orebody dips at 20-30 degrees. While in the south limb extension, the 25-30 m wide orebody dips at 45 to 50 degrees. This means the orebody has plunged and the geological disturbances are the main cause of the complex structure of the orebody. The present orebody in the south extremity is a part of trough formation due to the high stress and is the main reason for the friable of the ore. In this zone, the hanging wall is highly sheared to a distance of 8-10 m, while shear zones also exist in the footwall at a distance of 3-10 m. The orebody comprises banded rhodonite/manganese quartzite, while, the hanging wall formations are pink gneiss. The wall rocks are good and stable in most places except in the South limb extremity area.

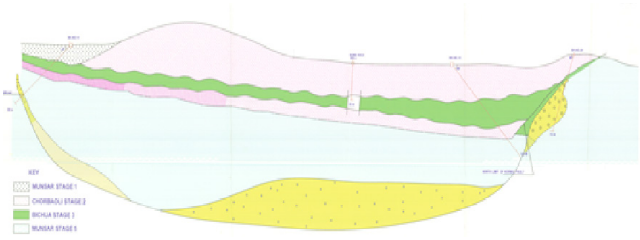

Figure 1. Part geological section of the studied area.

2.2 Stope Geometries

There are three levels of workings at 30 m regular intervals and the deepest 4 L is at approximately 185 m. With the success of 'Cable Bolting' practices, the stope length from the existing 30 m to 60 m for panel working of 3 stopes has been implemented (Figure 2). A Side Discharge Loader (SDL) has been introduced for mechanical handling of the RoM in the stope. Mechanized handling of RoM in stope by SDL has improved the face productivity in terms of output per man shift (OMS/T) from 3.5 T to 9 T. A stope block of 60 m length with left-out *in situ* rib and post pillars (for width >12 m) is mostly followed. A panel of 3 such stopes exist for 180 m strike length of the orebody including: (1) stope for mechanical handling of ROM by SDL with production drilling and blasting. (2) stopes for preparatory operations like hydraulic sand stowing, supported by cable and roof bolting.

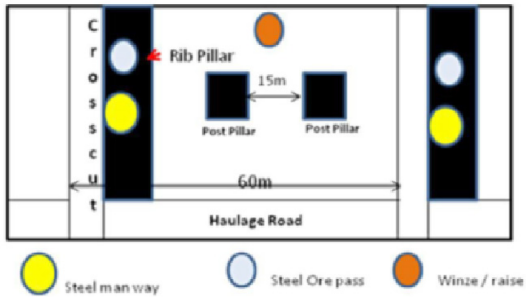

Figure 2. Conceptual stope geometries of the mine.

3.0 Experimental Blast Design and Monitoring

3.1 Blast Details

Test blasts were conducted in different stope levels and were monitored with compliance and advanced seismographs. The blasthole diameter was 32 mm and the explosive used was cartridge slurry (Neogel-80%). The blast holes were drilled with a jackhammer with a depth of 1.2 m. Blasting in 2.4 m × 2.1m galleries was carried out using the wedge-cut method. The plan and section of the blast design are provided in Figure 3.

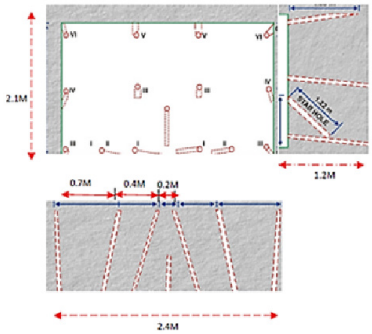

Figure 3. Drilling pattern and blast hole geometry (Wedge cut).

As mentioned earlier, the blast-induced ground vibrations were monitored by 2 seismographs at various monitoring stations at different distances from the blast site. The details of explosive charge configurations and the vibrations levels observed at different distances from the blast site are provided in Table 1.

4.0 Near Field Vibration Attenuation Analysis

Regression analysis of the blast data was attempted initially using a cube root scaled distance method. However as can be seen in Figure 4, R^2 was low at 0.54. The analysis pointed to the fact that the data in the model was bimodal and correspond to the measurements made near the stope and backfill material.

Keeping in view the above assertion, the data was split into two groups viz. that belonging to the stope area and another that belonging to the backfilled area. The separate regression of the data classified into two groups (Figure 5) revealed the following two equations (Eq. 1 and 2).

$V_{max} = 4438(D/Q^{1/3})^{-1.78}$ *with* R^2 *of 0.94 for the stope and footwall area ... (1)*

$V_{max} = 4695(D/Q^{1/3})^{-2.27}$ *with* R^2 *of 0.95 for the hangwall and backfill area ... (2)*

Where V_{max} *is the Peak Vector Sum in mm/s, D is the distance of the seismograph from the blast site in m and Q is the Maximum Charge per delay in kgs.*

In order to avoid possible blast-induced damage to the underground workings as well as in the case of adjacent backfilled areas, hanging wall, footwall, weak roof or pillars from the blasting site suitable safe charge/delay was

Table 1. Blast parameters from trial blasts conducted in the mine

Sl No.	Blast Location (Stope No.)	Total Explosive per round (kg)	Maximum charge per delay (kg)	Distance (m)	PVS* (mm/s)
1	8A -350 L	2.375	0.75	17	12.4
2	7A -350 L	2.375	0.75	16	8.18
3	6A -350 L	0.750	0.125	22	7.2
4	6D -350 L	0.875	0.125	16	6.14
5	SHR -350 L	0.500	0.125	15	3.27
	SHR -350 L		0.125	18	2.39
6	8C -350 L	0.875	0.125	13	0.852
	8C -350 L		0.125	18	0.75
7	07 -350 L	1.250	0.125	8	34.4
	07 -350 L		0.125	13	37.1
8	6E-350 L	1.000	0.125	13	1.39
	6E-350 L		0.125	18	0.75
9	6D-350 L	2.000	0.125	16	14.2
	6D-350 L		0.125	21	3.82

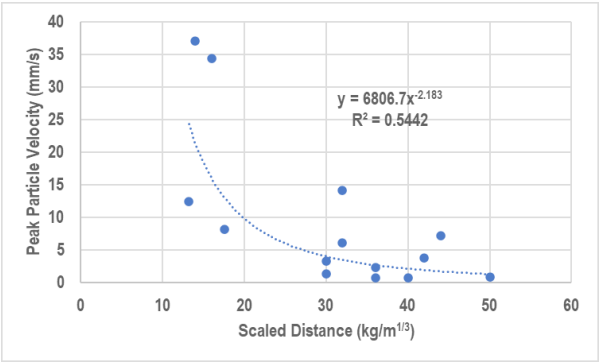

Figure 4. Regression results for the complete data set obtained from the blast monitoring.

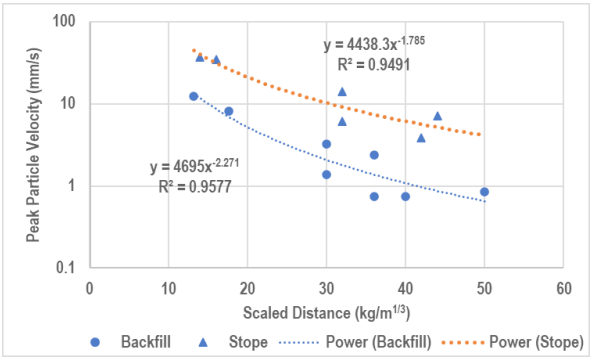

Figure 5. Vibration attenuation model and PVS vs Scaled Distances for backfill and stope areas.

worked out according to the distance and underground structures while using the criterion as defined below.

As per the guidelines of DGMS India[6] for underground workings, different vibration thresholds are specified for controlling the wall rock damage as given in Table 2. The rockmass in the current case is having RMR values of 35, 45 and 55 for hanging wall, stope and footwall, respectively. Accordingly, the DGMS vibration limits are highlighted in Table 2.

5.0 Damage/Pre-conditioning Prediction

Forsyth (1993) provided a method to determine the critical particle velocity for damage prediction as given in Eq. 3.

$$PPV_{crit} = \sigma_{t} \times v_{p}/E \quad (3)$$

Where σ_t is the tensile strength of the rock (MPa), E is the elastic Young's Modulus (MPa) and v_p is the compressional wave velocity (m/s).

The criterion above was invoked for the present case also. The critical values of particle velocity thus obtained are given in Table 3.

5.1 Holmberg and Persson Approach

After determining the site-specific attenuation constants, preliminary predictions of the extent of blast damage/pre-conditioning into hanging walls were made by applying the Holmberg and Persson model[7,8] as given in Figure 6, and by considering a site-specific critical ground vibration level in terms of peak particle velocity or PPV (mm/s) or damage threshold.

Table 2. A threshold value of vibration for the safety of underground' working (DGMS circular Tech. No. 6/2007)

RMR	A threshold value of vibration in terms of PPV (mm/s) in the case of Roof rock	A threshold value of vibration in terms of PPV (mm/s) in the case of Pillar rock
20-30	50	20
30-40	50-70	20-30
40-50	70-100	30-40
50-60	100-120	40-50
60-80	120	50

This means that a range of 20 to 120 mm/s can be used for different workings to fix the maximum charge per delay.

Table 3. Critical particle velocity for damage after Forsyth (1993)

Working	p-wave velocity m/s	Tensile strength (MPa)	E	PP_{crit}
Stope	6300	3.5	10	2205
Hangwall	5500	2.8	6.57	2344
Footwall	6300	5.6	10.38	2967

The values are practically good for estimating the total damage and failure and are on the higher side.

The tensile strength and modulus for the rockmass monitored are considered at 2.8 MPa and 6.57 GPa for HW, 3.5 MPa and 10 GPa for Ore and 5.6 MPa and 10.38 GPa for footwall, respectively. The compressional wave velocity was 6300 m/s in the case of footwall and ore rock and 5500 m/s in the case of hanging wall and is considered for the analysis. From the properties of rockmass and by adopting Eq. 3, the value of PPV critical or damage threshold for the various rockmasses determined is shown in (Figure 6). The possible extent of predicted blast-induced damage for various rockmass types is given in (Table 4).

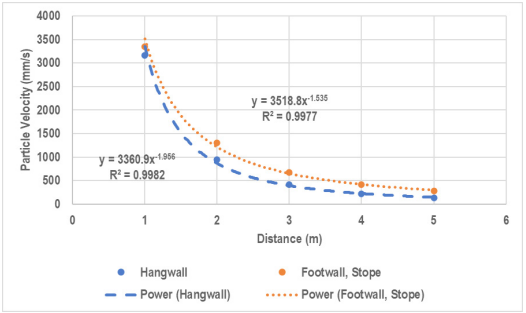

Figure 6. Damage/pre-conditioning prediction using the Holmberg and Persson approach.

Based on the above analysis, the PPV values predicted at a distance of 1 m from the blast hole are given in Table 4. The acceptable values from such equations can be achieved only beyond 4 m. This method, if deployed, may not be feasible as the maximum charge per delay predicted could be too less to allow blasting.

5.2 Blast Damage Index Approach4

The Blast Damage Index (BDI)[4] was also invoked to check the damage zone at different levels. The index is calculated as follows

$$BDI = \frac{PPV \times \rho_r \times c}{\kappa \times \sigma_{td}} \quad (4)$$

Where, PPV is the vector sum of peak particle velocity in m/s observed or calculated at a known distance, ρ_r is the density of the rock in g/cm³, c is the p-wave velocity in km/s, k is site quality constant = RMR/100, σ_{td} is dynamic tensile strength in MPa, estimated from the compressive strength of the rock.

From the properties of the rockmass as defined in section 5.1, and by adopting the above relationships (Eq. 1, 2 and 4), the value of BDI for various rockmasses determined is shown in Table 5. The possible extent of predicted blast-induced damage for various rockmass types.

The criterion on the basis of *BDI* provided by Yu and Vongpaisal[4] for rockmass damage is provided in Table 6.

The value of BDI = 0.5 was taken as a threshold criterion for all the workings in the present case as the workings are of temporary nature. This yielded threshold PPV values of 104, 390 and 155 mm/s for stope, footwall and hanging wall, respectively. Accordingly, using these values of PPV, the safe maximum charge per delay (Q_{max}) is determined using Eq. 1 and 2, for various distances from the blast site to control blast-induced damage to the underground workings is given in (Table 7).

The observations of the actual damage zone in the stope area are shown in Figure 7, which correlate well with the predicted values.

The values of Q_{max} thus obtained were deployed for blast design in the mine. It was observed that the damage levels are well corroborating with the damage predicted by BDI. Hence, the same was recommended for further operations. Some damage could be allowed as the workings are of temporary nature and in order to sustain the productivity of the mine.

Table 4. The extent of predicted blast-induced damage

Rock Type	PPV at 1 m
Hanging wall	3158
Footwall	3348
Ore	3158
Average for rock mass	

6.0 Conclusions

A comprehensive blast monitoring was carried out to investigate the extent of the blast-induced damage on the hanging wall, footwall and friable orebody in the

Table 6. Damage classification based on BDI as per Yu and Vongpaisal[4]

BDI	Type of damage to the rock mass
≤0.125	No damage
0.25	No noticeable damage
0.5	Minor or discrete scabbing effect
0.75	Moderate and discontinuous scabbing damage
1.0	Major and continuous scabbing failure
1.5	Severe damage to the entire opening
≥2.0	Major caving

Table 5. Blast Damage Index for different workings of the mine

Working	Rock	PPV mm/s	d (g/cc)	v_p (km/s)	RMR/100	σ_{td}	BDI	Type of damage predicted
Stope	Ore	20	4.4	6.3	0.495	11.55	0.10	No damage
		50	4.4	6.3	0.495	11.55	0.24	No noticeable damage
		104	4.4	6.3	0.495	11.55	0.50	Minor damage
Footwall	Gneiss	20	2.6	5.5	0.605	18.48	0.03	No damage
		50	2.6	5.5	0.605	18.48	0.06	No damage
		390	2.6	5.5	0.605	18.48	0.50	No noticeable damage
Hanging wall	Schist	20	2.1	5.5	0.385	9.24	0.06	No damage
		50	2.1	5.5	0.385	9.24	0.16	No damage
		155	2.1	5.5	0.385	9.24	0.50	No noticeable damage

Where PPV is the peak vector sum of the threshold for damage in mm/s, ρ_r is the density of rock in g/cm³, v_p is the p-wave velocity of the rock, RMR is the rock mass rating of the rock adjusted for support, σ_{td} is the dynamic tensile strength estimated from the tensile strength of the rock in MPa, BDI is the blast damage index. Highlighted values of PPV are the threshold values of damage to the rock. The values of 20 and 50 mm/s are taken for comparison from the DGMS criterion given in Table 2.

Table 7. Maximum charge delay calculations for use in different places of the mine

Working	Distance	Q_{max} (g), predicted	Q_{max} (g), recommended	Damage level
Hanging wall	1	4	63	Moderate
	2	29	63	Minor
	3	98	125	Minor
	4	231	125	No damage
	5	452	125	No damage
	6	781	125	No damage
Stope	1	7	63	Moderate
	2	52	63	Minor
	3	176	125	Minor
	4	416	250	No damage
	5	813	250	No damage
	6	1405	250	No damage
Footwall	1	37	63	Moderate
	2	299	125	No damage
	3	1008	250	No damage
	4	2388	250	No damage
	5	4665	250	No damage
	6	8061	250	No damage

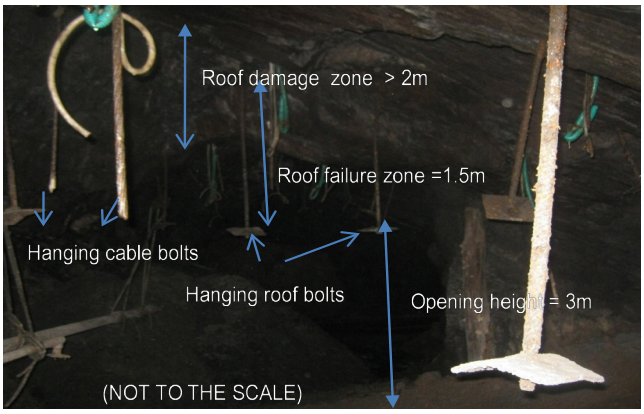

Figure 7. Correlations with field observations - Failure and damage zone at studied Mine.

cut and fill stoping operation. The damage prediction by Forsyth and Holmberg's approach was almost matching. However, these appear to be on the higher side as these were probably meant to calculate levels of total damage. The criterion suggested by DGMS seems to be on the very conservative side. Keeping in view the above, the BDI approach was taken up and a prediction of damage levels was made with its help. With the help of BDI worked for different workings of the mine, and by deploying some local adjustments the maximum charge per delay could be evaluated. This allowed for control of wall rock damage and also allowed to provide means to sustain the productivity of the mine. Further research in this direction is going on and is expected to provide better results with some refinements in the modelling procedure and damage calculations.

7.0 References

1. Villaescusa E, Onederra I, Scott C. Blast induced damage and dynamic behaviour of hangingwalls in bench stoping. Fragblast. 2004; 8. https://doi.org/10.1080/13855140512331389614
2. Drover C, Villaescusa E. A comparison of seismic response to conventional and face destress blasting during deep tunnel development. J Rock Mech Geotech Eng. 2019; 11. https://doi.org/10.1016/j.jrmge.2019.07.002
3. Raina AK, Chakraborty AK, Ramulu M, Jethwa JL. Rockmass damage from underground blasting, a literature review, and lab- And full-scale tests to estimate crack depth by ultrasonic method. Fragblast. 2000; 4:103-125. https://doi.org/10.1076/frag.4.2.103.7449
4. Yu TR, Vongpaisal S. New blast damage criteria for underground blasting. CIM Bull. 1996; 89:139-145.
5. Sheorey PR. Ground control in board and pillar mining. Dhanbad. 2008.
6. DGMS. A threshold value of vibration for the safety of underground working. India. 2007. https://elibrarywcl.files.wordpress.com/2015/02/dgms-tech-circular-no-06-of-2007-blast-induced-vibration.pdf
7. Onederra IA, Furtney JK, Sellers E, Iverson S. Modelling blast-induced damage from a fully coupled explosive charge. Int J Rock Mech Min Sci. 2013. https://doi.org/10.1016/j.ijrmms.2012.10.004
8. Persson PA, Holmberg R, Lee J. Rock blasting and explosives engineering. 1994.